EARTHQUAKE ENGINEERING AND STRUCTURAL DYNAMICS
Earthquake Engng Struct. Dyn. 2005; **34**:1551–1571
Published online 1 June 2005 in Wiley InterScience (www.interscience.wiley.com). DOI: 10.1002/eqe.492

Effect of peak ground velocity on deformation demands for SDOF systems

S. Akkar*,† and Ö. Özen

Earthquake Engineering Research Center, Department of Civil Engineering, Middle East Technical University, 06531 Ankara, Turkey

SUMMARY

The effect of peak ground velocity (PGV) on single-degree-of-freedom (SDOF) deformation demands and for certain ground-motion features is described by using a total of 60 soil site records with source-to-site distances less than 23 km and moment magnitudes between 5.5 and 7.6. The observations based on these records indicate that PGV correlates well with the earthquake magnitude and provides useful information about the ground-motion frequency content and strong-motion duration that can play a role on the seismic demand of structures. The statistical results computed from non-linear response history analyses of different hysteretic models highlight that PGV correlates better with the deformation demands with respect to other ground motion intensity measures. The choice of PGV as ground motion intensity decreases the dispersion due to record-to-record variability of SDOF deformation demands, particularly in the short period range. The central tendencies of deformation demands are sensitive to PGV and they may vary considerably as a function of the hysteretic model and structural period. The results provided in this study suggest a consideration of PGV as a stable candidate for ground motion intensity measure in simplified seismic assessment methods that are used to estimate structural performance for earthquake hazard analysis. Copyright © 2005 John Wiley & Sons, Ltd.

KEY WORDS: peak ground velocity; ground motion intensity measures; ground-motion features; SDOF deformation demand; hysteretic models

1. INTRODUCTION

The underlying principle in performance-based seismic design is to establish a consistent methodology on the exceeding probabilities of structural damage states (i.e. limit states) for a given seismic hazard level. The seismic hazard is quantified through a ground motion intensity measure (IM, e.g. peak ground acceleration PGA, spectral acceleration S_a, etc.) whereas the damage state is described in terms of an engineering demand measure (DM, e.g. maximum roof and interstorey drift, displacement ductility, etc.). The inherent uncertainties associated

*Correspondence to: S. Akkar, Earthquake Engineering Research Center, Department of Civil Engineering, Middle East Technical University, 06531 Ankara, Turkey.
†E-mail: sakkar@metu.edu.tr

Received 26 August 2004
Revised 8 February 2005
Accepted 8 February 2005

with the intensity and demand measures and their correlation/relevance for a specific structural response due to a particular ground motion type poses a significant debate for performance-based seismic engineering research. The proposed analytical methods should rigorously manifest the statistical relationship between the chosen IM and DM for reliable structural damage assessment, yet they should be practical and easily understood for engineering calculations. Within this scope a search for an elaborate IM that captures the prominent ground-motion features with smaller dispersions about the central tendency of DM (i.e. mean or median behaviour) is of prime importance for performance-based earthquake engineering.

Efforts in predicting DMs for structural systems deforming beyond their elastic limits are abundant in the literature. Most of these studies focus on the estimation of peak displacement ductility demand μ, the ratio of maximum inelastic deformation to yield deformation. The displacement ductility as a DM provides an estimate of peak non-linear deformation of a structural system and is usually related to the normalized yield strength R (ratio of elastic to yield strength of the structure). The studies by Veletsos and Newmark [1], Newmark and Hall [2, 3], Lai and Biggs [4], Elghadamsi and Mohraz [5], Riddell *et al*. [6–8], Nassar and Krawinkler [9], Miranda [10, 11], Vidic *et al.* [12], Ordaz and Pérez-Rocha [13], and Cuesta and Aschheim [14] may be cited among those that describe period-dependent rules (called as R–μ–T relations) for estimating the maximum deformation demands on SDOF systems. The common methodology in these relations is to develop period-dependent regression expressions for the central tendencies of DM by using the results provided from the SDOF non-linear response history analyses. The difference among these procedures, however, is the implementation of the IM parameter to the devised rule that predicts the target DM. Procedures proposed by Veletsos and Newmark [1], Newmark and Hall [2, 3], Riddell and Newmark [6], Vidic *et al*. [12], and Cuesta and Aschheim [14] consider the ratio of peak ground motion values (peak ground velocity to acceleration) to account for the frequency composition of ground motion record on the central tendency of DM. Miranda [10, 11] considered the influence of site condition, magnitude and epicentral distance on the mean DM. The proposed R–μ–T relationship by Ordaz and Pérez-Rocha [13] essentially used peak ground displacement to estimate the mean maximum deformation demands for non-linear oscillator response. Recently, Miranda [15] and Ruiz-García and Miranda [16] provided period-dependent direct displacement modification factors for a given μ or R to predict the maximum inelastic deformation demands on SDOF systems using their elastic counterparts. The derived regression relationships are based on comprehensive ground-motion data sets and consider the influence of site condition, magnitude and closest source-to-site distance on deformation demands. Miranda [15] and Ruiz-García and Miranda [16] also provided the dispersion statistics about the central tendency of DMs and indicated that the dispersion can vary significantly depending on the period of vibration, level of inelastic deformation and local site conditions. More recently, Farrow and Kurama [17] conducted detailed statistical analyses on other DMs to quantify cumulative damage, hysteretic energy and residual deformation of structural systems subjected to earthquake ground motions. The large ground-motion data set used by Farrow and Kurama [17] is comprised of stiff and soft soil records with different levels of exceeding probabilities for low and high seismic regions in the U.S. Similar to the other studies cited above, Farrow and Kurama [17] derived regression equations for the central tendencies of the considered demand indices using SDOF non-linear response history analyses. As part of their study, the authors indicated that the dispersions around the central tendencies of DMs are affected by the ground motion intensities and vary erratically by means of vibration period and inelastic deformation level.

More detailed information on IM parameters and their intricate relationship with the selected DM has been revealed by the probability-based damage assessment research. Shome *et al.* [18] indicated that the dispersion about median DM predictions reduce when ground-motion bins of narrow magnitude and distance interval are normalized (or scaled) to the bin-median spectral acceleration at the fundamental period of structure (i.e. $S_a(T_1)$) under consideration. Cordova *et al.* [19] proposed a two parameter IM that accounts for the period shift resulting from inelastic structural response. The proposed IM is based on the spectral acceleration ratio of fundamental mode period ($S_a(T_1)$) to relatively longer period ($S_a(T_f)$) that mimics the non-linear structural behaviour due to inelastic response. The fundamental mode spectral acceleration approach ($S_a(T_1)$) for defining the IM is also used by Krawinkler *et al.* [20] to explore the variation of storey drift and storey ductility DMs under specific ground motion records. As part of this extensive research, Krawinkler *et al.* [20] concluded that firm site ground motions with magnitudes ranging between 5.5 and 7.0 and distances more than 15 km from the fault rupture (designated as 'ordinary records') have frequency characteristics insensitive to magnitude and distance. This concluding remark is used by the authors to describe the unbiased central tendency of the DM parameters as a function of a single IM (i.e. $S_a(T_1)$) for regular frame structures deforming primarily in the first mode. A recent study conducted by Giovenale *et al*. [21] proposed probability-based methods to test the 'efficiency' and 'sufficiency' of alternative IMs (defined as *original* and *candidate* ground motion intensity indices in the referred study) for a chosen DM. The dispersion comparison of the DM conditional to the alternative IMs is the criterion for deciding on the most appropriate IM. It should be noted that the common IM used in the probability-based damage assessment procedures (such as the ones cited above) is either a component of S_a or PGA as they make use of probabilistic seismic hazard curves and ground-motion prediction equations (attenuation relationships) that are derived in detail for S_a and PGA due to the traditional code approach.

Over the last decade, studies on relating the structural damage to alternative ground motion intensities have accelerated among the engineering and seismological community. Unexpected structural/non-structural damage due to large near-fault earthquakes that have occurred in densely built areas and a large number of ground motions recorded during these earthquakes stimulated these efforts. Wald *et al.* [22] investigated the correlation between the Modified Mercalli Intensity (MMI) and PGA and PGV. Based on the instrumental data obtained from 8 California earthquakes, the study by Wald *et al.* [22] revealed that PGV represents a better correlation for larger MMI values. A similar study by Wu *et al.* [23] found comparable results to Wald *et al.* [22] by using the ground motion data from the 1999 Chi-Chi, Taiwan, earthquake. Another observation highlighted by Wu *et al.* [23] is that between PGA and PGV, the latter IM has a stronger correlation with the earthquake magnitude. As a matter of fact, earlier work (e.g. References [24, 25]) has also emphasized the significance of ground velocity as an IM on structural response. These studies introduced the incremental velocity concept (pulse area under acceleration time series) specific to near-fault ground motions with pulse signals and showed the increasing structural damage for increasing incremental velocity value. The conclusions derived in these and similar studies could not be implemented in the wide array of engineering calculations due to the lack of PGV-based ground-motion prediction equations that would promote PGV as a well-recognized IM. (Until recently, the common references for PGV-based ground-motion prediction equations were limited only to those of Joyner and Boore [26] and Campbell [27, 28]). Recent seismological studies have premised PGV-based

prediction equations due to the inadequacy of using solely PGA or S_a for design and seismic performance assessment of structures [29–33]. However, these seismologically compelled studies should be incorporated by other studies that provide comprehensive information for the suitability of PGV as an IM on the chosen DM.

The objective of this study is to scrutinize the properties of PGV intensity measure for the description of prominent ground-motion features and its corresponding effects on SDOF deformation demands. A ground-motion data set of 60 soil site records with closest source-to-site distances less than 23 km and moment magnitudes (**M**) ranging between 5.5 and 7.6 is divided into three PGV bins. Each ground motion bin constitutes 20 records that cover the PGV values of less than 20, 20–40, and 40–60 cm/s, respectively. The ground motions do not contain pulse signals that may introduce bias in the conclusions exclusively derived for the direct effect of PGV on the ground motion features and DMs. Therefore, the results and conclusions presented should not be generalized for the pulse dominant waveforms that are mostly observed in near-fault records with forward directivity. Limited to the data set used in this study, the correlations between PGV and magnitude, ground-motion frequency content, and strong-motion duration are presented. Non-linear oscillator response history analyses are conducted using different hysteretic models to obtain the period-dependent central tendency of maximum SDOF deformation demand (DM selected in this study) for the subject PGV bins. Using the non-linear response history analyses results, period-dependent correlation coefficients are computed between PGV and maximum SDOF deformation demands at various inelastic deformation levels. Similar correlation coefficients are also computed for alternative IMs to compare and quantify the capability of PGV as an intensity measure on maximum SDOF deformation demands. The dispersion around the central tendency of the selected DM is described to see the role of PGV on the uncertainties associated with the subject DM due to record-to-record variability. The discussions presented in this paper are believed to be useful for future studies that aim to provide elaborate methodologies for reliable structural damage assessment in relation to seismic hazard.

2. GROUND MOTION DATA

Tables I–III list the important features of ground motions used in this study. Each table presents a total of 20 records that are grouped for a pre-determined PGV range to assess the influence of this IM on certain ground-motion parameters and on SDOF deformation demands. The first ground-motion bin that consists of records having PGV values less than 20 cm/s is listed in Table I. The second and third ground-motion bins are comprised of records with PGV values ranging between 20–40 and 40–60 cm/s and they are shown in Tables II and III, respectively. The records represent soil site recordings and their site information is obtained from the COSMOS (http://www.cosmos-eq.org) Virtual Data Center where the data is downloaded. Given the site information presented in Tables I–III, the ground motions represent records of site classes C and D according to the current seismic provisions in the U.S. [34]. The filtering information given for the downloaded data indicated that, on average, the accelerograms are low-cut filtered by corner frequencies between 0.1 and 0.2 Hz except for the digital 1999 Chi-Chi, Taiwan, earthquake records that are processed by corner frequencies of 0.04 Hz. This information is used in defining the period bound for non-linear response history computations. The velocity time series of each record is examined in order to exclude

Table I. Ground motion bin for PGV values less than 20 cm/s.

Earthquake	M	Fault	Station	Comp.	Site*	d (km)	PGA (cm/s^2)	PGV (cm/s)	PGD (cm)
Whittier Narrows, 10/01/87	6.1	Thrust/reverse	7420 Jaboneria, Bell Gardens	S27W	Alluvium (Q-Qym)	16.4	89.8	2.7	0.4
Morgan Hill, 04/24/84	6.1	Strike slip	Gilroy–Gavilan College	67	Terrace deposit over sandstone	13.2	95.0	3.4	0.5
Coyote Lake, 08/06/79	5.7	Strike slip	SJB Overpass, Bent 3	67	Alluvium	17.2	84.6	4.7	0.7
Morgan Hill, 04/24/84	6.1	Strike slip	Gilroy #2	0	Alluvium	11.8	153.7	5.0	1.1
Morgan Hill, 04/24/84	6.1	Strike slip	Gilroy #7	90	Alluvium over sandstone	7.9	111.5	5.8	0.6
North Palm Springs, 07/08/86	6.2	Strike slip	Fun Valley	45	Q	12.7	123.5	6.1	1.0
Whittier Narrows, 10/01/87	6.1	Thrust/reverse	200 S. Flower, Brea, CA	N20E	Q-Qof	22.2	109.4	7.1	1.3
North Palm Springs, 07/08/86	6.2	Strike slip	Fun Valley	135	Q	12.7	123.0	9.5	1.4
Livermore, 01/27/80	5.8	Strike slip	Morgan Territory Park	265	Class C	8.0	242.7	11.0	1.4
Imperial Valley, 10/15/79	6.5	Strike slip	Borchard Ranch, El Centro Array #1	S50W	Alluvium (Q)	22.6	121.1	10.4	7.4
Morgan Hill, 04/24/84	6.1	Strike slip	Gilroy #6	0	Silty clayover sandstone	6.1	214.8	11.3	1.8
Morgan Hill, 04/24/84	6.1	Strike slip	Gilroy #3	90	Alluvium	10.3	189.8	11.9	2.6
Loma Prieta, 10/18/89	7.0	Oblique	Gilroy #6 - San Ysidoro	0	Silty clayover sandstone	12.2	112.2	13.1	5.0
Loma Prieta, 10/18/89	7.0	Oblique	Gilroy #6 - San Ysidoro	90	Silty clayover sandstone	12.2	166.9	13.9	3.4
Coyote Lake, 08/06/79	5.7	Strike slip	Gilroy Array No. 3 Sewage Treatment	50	Alluvium	6.0	252.4	16.9	3.7
Imperial Valley, 10/15/79	6.5	Strike slip	Parachute Test Facility, El Centro	N45W	Q	10.4	197.6	17.3	10.9
Imperial Valley, 10/15/79	6.5	Strike slip	Calexico Fire Station	N45W	Alluvium (Q)	10.4	197.6	18.9	15.2
Imperial Valley, 10/15/79	6.5	Strike slip	Casa Flores, Mexicali	0	Alluvium	9.8	236.8	19.3	7.2
Livermore, 01/24/80	5.5	Strike slip	Livermore VA Hospital	128	Alluvium;600m; Sandstone	No Inf	121.7	17.4	3.4
Livermore, 01/24/80	5.5	Strike slip	Livermore VA Hospital	38	Alluvium;600m; Sandstone	No Inf	180.3	17.9	2.3

Abbreviations for site conditions: Q : Quaternary ($V_s = 333$ m/s); T : Tertiary ($V_s = 406$ m/s); Qym : Holocene, medium-grained sediment; Qyc : Holocene, coarse grained sediment; Qof : Pleistocene, fine-grained sediment; Qom : Pleistocene, medium-grained sediment; Class C: 360 m/s $< V_s <$ 750 m/s; Class D: 180 m/s $< V_s <$ 360 m/s.

Table II. Ground motion bin for PGV values between 20 and 40 cm/s.

Earthquake	M	Fault	Station	Comp.	Site*	d (km)	PGA (cm/s^2)	PGV (cm/s)	PGD (cm)
Whittier Narrows, 10/01/87	6.1	Thrust/reverse	Los Angeles- Obregon Park	360	Alluvium (Q-Qom)	14.2	420.1	21.8	2.8
Northridge, 01/17/94	6.7	Thrust/reverse	Los Angeles - UCLA Grounds	360	Alluvium (Q-Qom)	22.9	464.6	21.9	7.3
Northridge, 01/17/94	6.7	Thrust/reverse	Los Angeles - UCLA Grounds	90	Alluvium (Q-Qom)	22.9	272.4	22.0	4.0
Imperial Valley, 10/15/79	6.5	Strike slip	Community Hospital, Keystone Rd., El Centro Array #10	S50W	Alluvium; more than 300m	8.7	117.3	22.9	13.3
Loma Prieta, 10/18/89	7.0	Oblique	Gilroy - Gavilan College	337	Terrace deposit over sandstone	3.0	310.0	23.0	4.8
Northridge, 01/17/94	6.7	Thrust/reverse	6850 Coldwater Canyon Ave., North Hollywood	S00W	Alluvium (Q-Qyc)	12.5	296.0	23.1	10.0
Imperial Valley, 10/15/79	6.5	Strike slip	Aeropuerto Mexicali	315	Deep Alluvium	3.2	249.9	23.9	5.4
Northridge, 01/17/94	6.7	Thrust/reverse	Los Angeles, Brentwood V.A. Ho	195	Alluvium (Q-Qom)	23.1	182.1	24.0	5.4
Parkfield, 06/27/66	6.1	Strike slip	Chalome, Shandon, Array No. 5	N85E	Alluvium; Sandstone (Q)	7.1	425.7	25.4	7.1
Whittier Narrows, 10/01/87	6.1	Thrust/reverse	7420 Jaboneria, Bell Gardens 5	N63W	Alluvium (Q-Qym)	16.4	215.9	28.0	5.0
Loma Prieta, 10/18/89	7.0	Oblique	Gilroy - Gavilan College	67	Terrace deposit over sandstone	3.0	349.1	28.9	5.8
Imperial Valley, 10/15/79	6.5	Strike slip	Casa Flores, Mexicali	270	Alluvium	9.8	414.7	31.5	7.7
Coyote Lake, 08/06/79	5.7	Strike slip	Gilroy Array No. 2	140	Alluvium	6.0	248.9	31.9	5.3
Imperial Valley, 10/15/79	6.5	Strike slip	Keystone Rd., El Centro Array #2	S40E	Alluvium (Q)	16.2	309.4	32.7	15.0
Loma Prieta, 10/18/89	7.0	Oblique	Gilroy #2 - Hwy 101/Bolsa Rd	0	Alluvium	4.5	344.2	33.3	6.7
Loma Prieta, 10/18/89	7.0	Oblique	Gilroy #3 - Gilroy Sewage Plant	0	Alluvium	6.3	531.7	34.5	7.4
Loma Prieta, 10/18/89	7.0	Oblique	Saratoga - 1 Story School Gym	270	Alluvium	13.7	347.3	37.2	7.8
Imperial Valley, 10/15/79	6.5	Strike slip	Anderson Rd., El Centro Array #4	S40E	Alluvium; more than 300m	8.3	480.8	38.1	22.0
Loma Prieta, 10/18/89	7.0	Oblique	Gilroy #2 - Hwy 101/Bolsa Rd	90	Alluvium	4.5	316.3	39.2	10.9
Morgan Hill, 04/24/84	6.1	Strike slip	Halls Valley	240	Alluvium	2.5	305.8	39.6	6.6

Abbreviations for site conditions: Q : Quaternary ($V_s = 333$ m/s); T : Tertiary ($V_s = 406$ m/s); Qym : Holocene, medium-grained sediment; Qyc : Holocene, coarse grained sediment; Qof : Pleistocene, fine-grained sediment; Qom : Pleistocene, medium-grained sediment.

Table III. Ground motion bin for PGV values between 40 and 60 cm/s.

Earthquake	M	Fault	Station	Comp.	Site*	d (km)	PGA (cm/s^2)	PGV (cm/s)	PGD (cm)
Chi-Chi, Taiwan, 09/20/99	7.6	Thrust/reverse	Taichung - Chungming School, TCU051	360	Class D	7.0	230.0	40.6	42.5
Chi-Chi, Taiwan, 09/20/99	7.6	Thrust/reverse	Taichung - Taichung City, TCU082	360	Class D	4.5	182.1	41.0	39.3
Imperial Valley, 10/15/79	6.5	Strike slip	Dogwood Rd., Diff. Array, El Centro	NS	Alluvium (Q)	5.6	473.6	41.1	16.3
Imperial Valley, 10/15/79	6.5	Strike slip	Aeropuerto Mexicali	45	Deep alluvium	3.2	284.9	42.0	10.1
Chi-Chi, Taiwan, 09/20/99	7.6	Thrust/reverse	Chiayi - Meishan School, CHY006	360	Class D	14.5	351.8	42.1	16.4
Cape Mendocino, 04/25/92	7.0	Thrust/reverse	Rio Dell-101/Painter St. Overpass	360	Class C	18.5	538.5	42.6	13.4
Landers, 06/28/92	7.3	Strike slip	Joshua Tree-Fire Station	90	Shallow alluvium over granite bedrock (Q)	10.0	278.4	42.7	15.7
Imperial Valley, 10/15/79	6.5	Strike slip	Bonds Corner	140	Alluvium (Q)	4.4	578.0	44.3	15.0
Imperial Valley, 10/15/79	6.5	Strike slip	Bonds Corner	230	Alluvium (Q)	4.4	762.4	45.0	15.1
Imperial Valley, 10/15/79	6.5	Strike slip	McCabe School, El Centro Array #11	S50W	Alluvium (Q)	12.4	362.5	45.2	22.3
Imperial Valley, 10/15/79	6.5	Strike slip	Community Hospital, Keystone Rd., El Centro Array #10	N40W	Alluvium; more than 300m (Q)	8.7	226.6	46.0	26.7
Cape Mendocino, 04/25/92	7.0	Thrust/reverse	Petrolia	0	Alluvium	9.5	578.1	48.3	15.2
Imperial Valley, 10/15/79	6.5	Strike slip	James Rd., El Centro Array #5	S40E	Alluvium; more than 300m (Q)	5.2	539.8	49.7	40.8
Kocaeli 8/18/99	7.4	Strike slip	Duzce	SN	Alluvium	17.1	307.8	50.7	35.8
Northridge, 01/17/94	6.7	Thrust/reverse	Pacoima-Kagel Canyon	360	Sandstone (T)	10.6	424.2	50.9	6.6
Duzce, 11/12/99	7.1	Strike slip	Bolu	NS	Alluvium	20.4	722.1	55.2	24.4
Loma Prieta, 10/18/89	7.0	Oblique	Corralitos-Eureka Canyon Rd.	0	Landslide deposits	2.8	617.7	55.2	9.5
Northridge, 01/17/94	6.7	Thrust/reverse	14145 Mulholland Dr., Beverly Hills, CA	N09E	Class D	19.6	419.3	57.9	15.0
Northridge, 01/17/94	6.7	Thrust/reverse	17645 Saticoy St.	S00E	Class D	13.3	428.7	59.8	17.6
Northridge, 01/17/94	6.7	Thrust/reverse	7769 Topanga Canyon Blvd., Canoga Park	S16W	Alluvium (Q-Qym)	15.7	381.0	59.8	12.4

Abbreviations for site conditions: Q : Quaternary ($V_s = 333$ m/s); T : Tertiary ($V_s = 406$ m/s); Qym : Holocene, medium-grained sediment; Qyc : Holocene, coarse grained sediment; Qof : Pleistocene, fine-grained sediment; Qom : Pleistocene, medium-grained sediment; Class C: 360 m/s $< V_s <$ 750 m/s; Class D: 180 m/s $< V_s <$ 360 m/s.

ground motions with pulse signals, as such records have distinct effects on the linear/non-linear structural response and they can mask/intervene the salient features of PGV both for ground-motion parameters and demand measures [35, 36]. The upper and lower limits of the moment magnitude and closest source-to-site distances (d) for the ground motions are $5.5 \leqslant \mathbf{M} \leqslant 7.6$ and $2.5\,\text{km} \leqslant d \leqslant 23\,\text{km}$, respectively. These ground motions can generically represent a near-fault data set of moderate to severe events that do not exhibit strong pulse effects due to forward directivity or any other seismological and geological complexity.

3. EFFECT OF PGV ON GROUND-MOTION PARAMETERS

Among particular ground-motion parameters, the earthquake magnitude, ground-motion duration and frequency composition of ground motion can provide comprehensive information on the earthquake hazard. A good correlation of these parameters with the chosen IM can be used to portray a proper description of demand changes on structural systems. Figure 1(a) displays the magnitude versus PGV for the ground motions presented in this study. The ground-motion bins are shown by different symbols for a clear observation of PGV variation with magnitude. The dark solid lines are the mean magnitude values computed for each ground-motion bin. The variation of earthquake magnitude with respect to PGV has a trend indicating that large magnitude events are more likely to produce ground motions with higher velocities. The higher expectation of large deformation demands for large magnitude events and the observations from Figure 1(a) can be interpreted as increased damage in structures that are subjected to ground motions with large velocity. This issue is addressed in the following section while discussing the sensitivity of SDOF deformation demands to different PGV levels.

Figure 1(b) displays a similar scatter plot as in Figure 1(a) for the variation of ground-motion duration with respect to PGV. The effective ground-motion duration (T_{eff}) definition of Bommer and Martínez-Periera [37] is used for the computation of strong ground shaking interval for each record. This definition is based on the Arias intensity that uses the accumulated ground motion energy. The effective durations are presented as the percentage of the

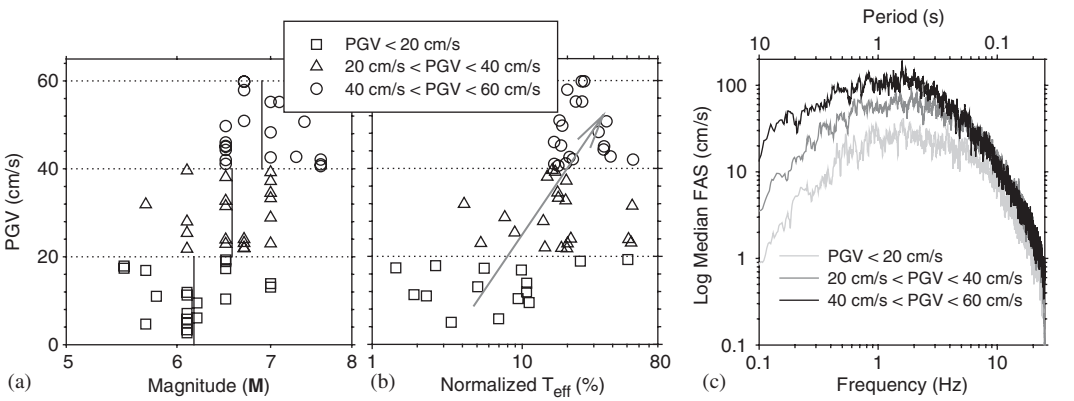

Figure 1. Variations of: (a) magnitude; (b) effective ground-motion duration; and (c) frequency composition with respect to PGV.

total record length for each ground motion in order to eliminate the discrepancies in T_{eff} due to the vast variation of recording durations among the ground motions. The scatter plots in Figure 1(b) show that the effective durations tend to increase for larger PGV particularly when the peak velocity amplitudes are greater than 20 cm/s. This observation can be important for post-yielding structures as longer effective duration may provoke the strength deterioration that could influence the deformation demand on structures.

The effect of PGV on the ground-motion frequency content is presented in Figure 1(c) by plotting the median Fourier amplitude spectrum (FAS) for the three ground-motion bins of different PGV ranges. The results are plotted for a frequency range of 0.1 Hz (10.0 s) to 25 Hz (0.04 s) considering the limitations imposed by the low-cut filter frequencies described in the preceding section. The Fourier amplitude spectrum gives a direct measure for the ground-motion frequency variation as a function of PGV. The plots indicate that there is a prominent PGV effect in the lower frequencies (i.e. in the longer periods) where the frequency content of ground motions imposing high velocities become notably rich. This observation was one of the fundamental remarks made by Newmark and Hall [3] and essentially can be related to the variation in SDOF deformation demands as will be discussed in the next section.

4. EFFECT OF PGV ON SDOF DEFORMATION DEMANDS

The previous section presented some elementary features of PGV on certain ground-motion parameters by using simple statistics. This section combines the observations made in the preceding section with the results of non-linear SDOF response history analyses to give a broader view for the role of PGV as an IM on deformation demand. The non-linear response history analyses are conducted for elastoplastic, modified Clough [38] and modified Takeda [39] hysteretic models to simulate different structural response under earthquake excitation. The critical damping is taken as 5-per cent for all response history computations. The results are presented for the mean variation of maximum SDOF deformations computed for each PGV-based ground-motion bin as a function of constant ductility μ and constant normalized strength ratio R. The displacement ductility and normalized strength displacement spectra provide distinct information for the deformation demands on structures that can guide the engineer for the preliminary design of new structures or for the seismic performance evaluation of existing structures, respectively. (The reader is referred to Miranda [15] and Ruiz-García and Miranda [16] for a broader discussion on the merits of constant ductility and constant normalized strength spectra.)

4.1. Sensitivity of spectral displacements to PGV

Figure 2 presents the mean maximum SDOF deformation demands (spectral displacements S_{d}) for the ground-motion bins used in this study. The non-linear maximum deformations are computed by using elastoplastic hysteretic model for a period range of 0.1–4.0 s that is consistent with the filter corner frequencies of the processed data. The results are presented for displacement ductility and normalized strength ratios ranging from 1 (i.e. elastic deformation demand) to 8. The first row in Figure 2 displays the results for constant ductility ratio whereas the second row shows the spectral displacements for normalized strength ratio R. The grey dotted lines in these plots approximately show the spectral corner periods T_{c} that divide the spectral

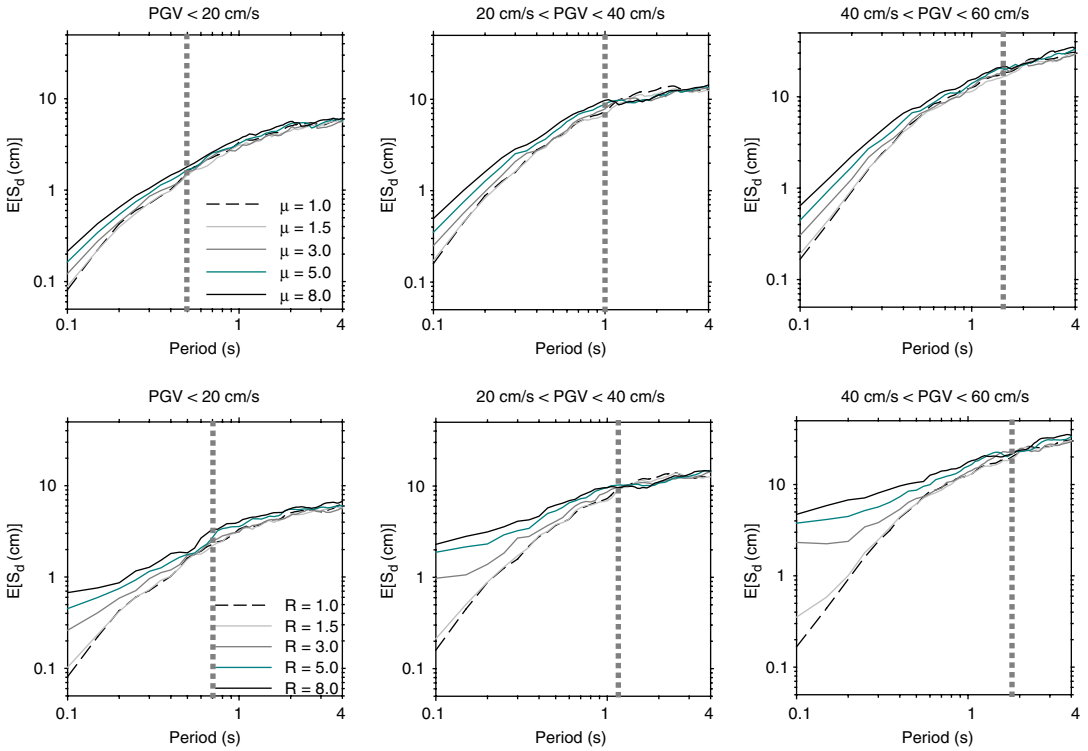

Figure 2. Effect of PGV on spectral displacements for constant μ and R.

regions where the so-called 'equal displacement' rule is applicable from those where this rule is not valid. The major observation from Figure 2 is the consistently increasing spectral displacements with the increase in PGV levels. Considering the fairly good correlation of PGV with earthquake magnitude, which is an important parameter in seismic hazard analysis, together with this information it can lead to a conclusion that PGV intensity measure can be a refined predictor of deformation demand on structures. The dependence of these conclusions on the selected bin size is addressed in Figure 3 by repeating the same computations for alternative ground-motion bins. Using 30 cm/s as the limiting PGV value, the first alternative bin consists of 31 records with PGV <30 cm/s whereas the second alternative bin is assembled by the remaining 29 records with PGV >30 cm/s. The mean S_d curves for constant μ and R levels in Figure 3 also show a consistent increase with increasing PGV levels. Comparisons between Figures 2 and 3 also reveal that PGV <30 cm/s bin yields mean S_d values larger than those computed for the PGV <20 cm/s bin. Similarly, mean S_d values pertaining to the PGV >30 cm/s bin are larger than the ones presented for the 20 cm/s $<$ PGV <40 cm/s bin. It is noted that mean non-linear deformation demand variation for different PGV levels in Figures 2 and 3 is not the same for constant μ and R spectra. This is due to the underlying deformation demand computation principles for constant ductility and normalized strength ratio. The constant ductility deformation demands are calculated for a limiting displacement ductility ratio whereas the computed deformation demands are not restrained in constant R

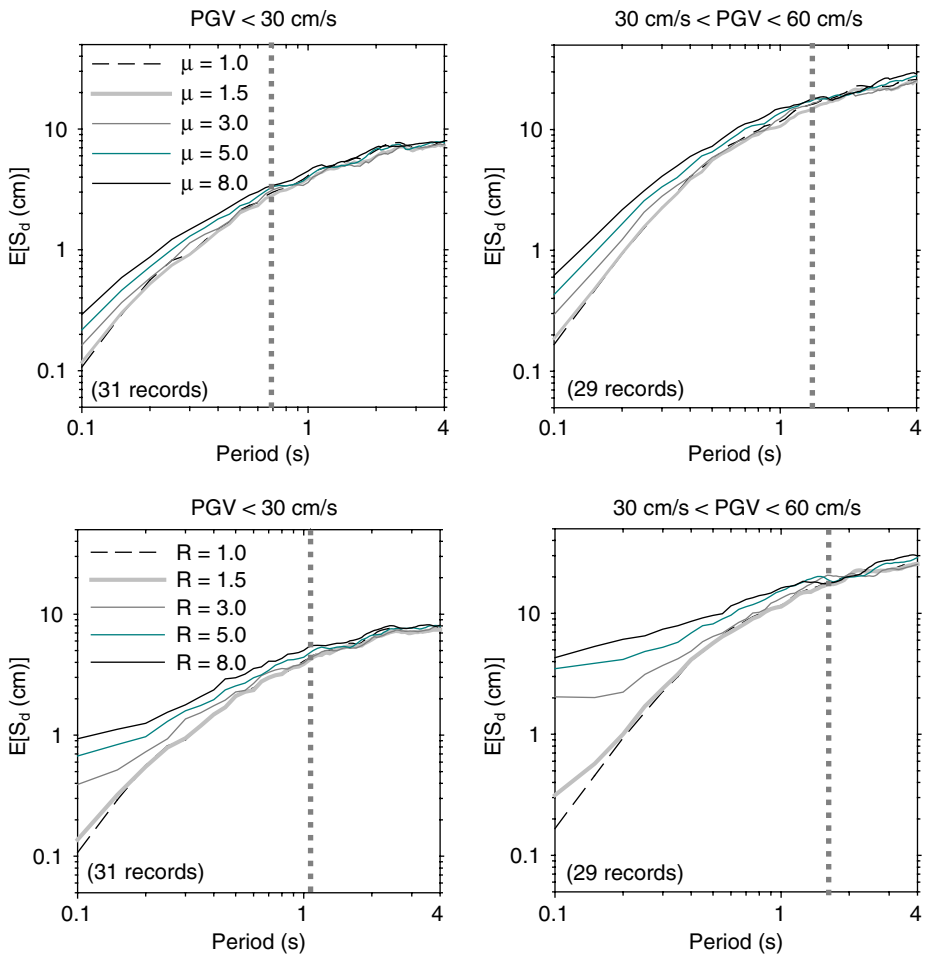

Figure 3. Effect of PGV on constant μ and R displacement spectra for alternative bin sizes.

spectra. As the periods shift towards shorter spectral regions, the deformation demands change substantially at different levels of the normalized strength ratio R. This should be a serious concern for the seismic performance assessment of existing structures prone to ground motions with high velocity.

Another important observation from Figures 2 and 3 is the sensitivity of T_c for the 'equal-displacement' rule. The previous research showed that T_c strongly depends on the site conditions (e.g. References [11, 15, 16]), however, based on the fairly similar site conditions for the ground motions presented, the results of this study have revealed that PGV itself is also an effective parameter to account for the changes in T_c. In Figure 2 the corner period for the highest PGV bin (i.e. records with $40\,\text{cm/s} < \text{PGV} < 60\,\text{cm/s}$) is approximately 2.5 times larger than the corner period of the ground-motion bin with $\text{PGV} < 20\,\text{cm/s}$ both for displacement ductility and normalized strength deformation demands. It should also be noted that the

variation of T_c differs for constant μ and R displacement spectra. The corner periods for constant ductility deformation demands are relatively shorter than those of the constant strength deformation demands at all PGV levels. The observations on the sensitivity of ground-motion frequency content to PGV that is discussed in the previous section and the variation of T_c with respect to different PGV levels are complementary features of PGV suggesting its consideration as a fairly effective intensity measure for the deformation demand on structures.

An independent ground-motion data set from the 1994 Northridge earthquake is used to verify the above remarks on the sensitivity of SDOF deformation demands to PGV that are described by using the particular ground-motion ensemble in this study. Figure 4 displays the mean PGA and PGV contour maps for the horizontal ground motion components of the 89 recording stations deployed around the Los Angeles metropolitan area that were triggered during the 1994 Northridge earthquake. The locations of the recording stations are shown by dark square boxes on these maps. Similar to the ground motions used in this study, these records have been downloaded from the COSMOS Virtual Data Center. The figure also presents the mean spectral displacement contours of the same horizontal components computed at particular periods ($T = 0.3,\ 0.5$, and 1.0 s) for normalized strength ratios $R = 2,\ 4$, and 8. The spectral displacements are computed using the elastoplastic hysteretic model. The selected periods fairly cover the spectral range where the spectral displacements are sensitive to the changes in R as discussed in Figures 2 and 3. This way the variation of S_d as a function of PGA or PGV can be observed in detail that would also yield a better comparison for the sensitivity of deformation demands to these alternative IMs. The spectral displacement contour maps are organized such that the pertinent maps for each particular period are presented row-wise whereas the column-wise spectral displacement maps correspond to different R values. The darker contours indicate higher mean peak ground values and spectral displacements. The contours are divided into equal number of intervals in each map to facilitate the comparisons between these two alternative IMs and the SDOF deformation demands. A better colour match between a peak ground value map and the spectral displacement maps would be the indication of deformation demand sensitivity to that IM. The comparisons between the mean PGA and spectral displacement contour maps show that at very short periods and low R values (i.e. short and stiff structures with relatively higher lateral strength capacities), the deformation demands resemble a good match for sites where mean PGA becomes maximum. The agreement between mean PGA and S_d diminishes as the inelastic level increases and the vibration period shifts to longer values. In particular, for $T > 0.5$ s and $R > 4$, the deformation demands reach their maxima for sites where mean PGA attains relatively moderate values. This phenomenon is also observed for $T > 0.3$ s and $R > 4$ (i.e. short and stiff structures with relatively lower lateral strength capacities) where sites with high deformation demands do not agree with the sites that experience very large ground acceleration. The comparisons between the mean PGV and spectral displacement contours reveal a fairly good overall agreement with respect to the performance of PGA. In particular, the contour maps of mean PGV and spectral displacements correlate well for higher inelastic levels (i.e. higher R values). The agreement between PGV and spectral displacements is more notable as the vibration period attains larger values. As a matter of fact, similar spectral displacement contour maps at higher periods show a very good correlation with the changes in PGV intensity that fortifies this observation. The sensitivity of deformation demands to PGV is also comparable to the performance of PGA for short-period oscillators with high lateral strength capacities (e.g. $R = 2,\ T = 0.3$ and 0.5 s cases in Figure 4). In brief, the discussions based on this independent ground-motion data set

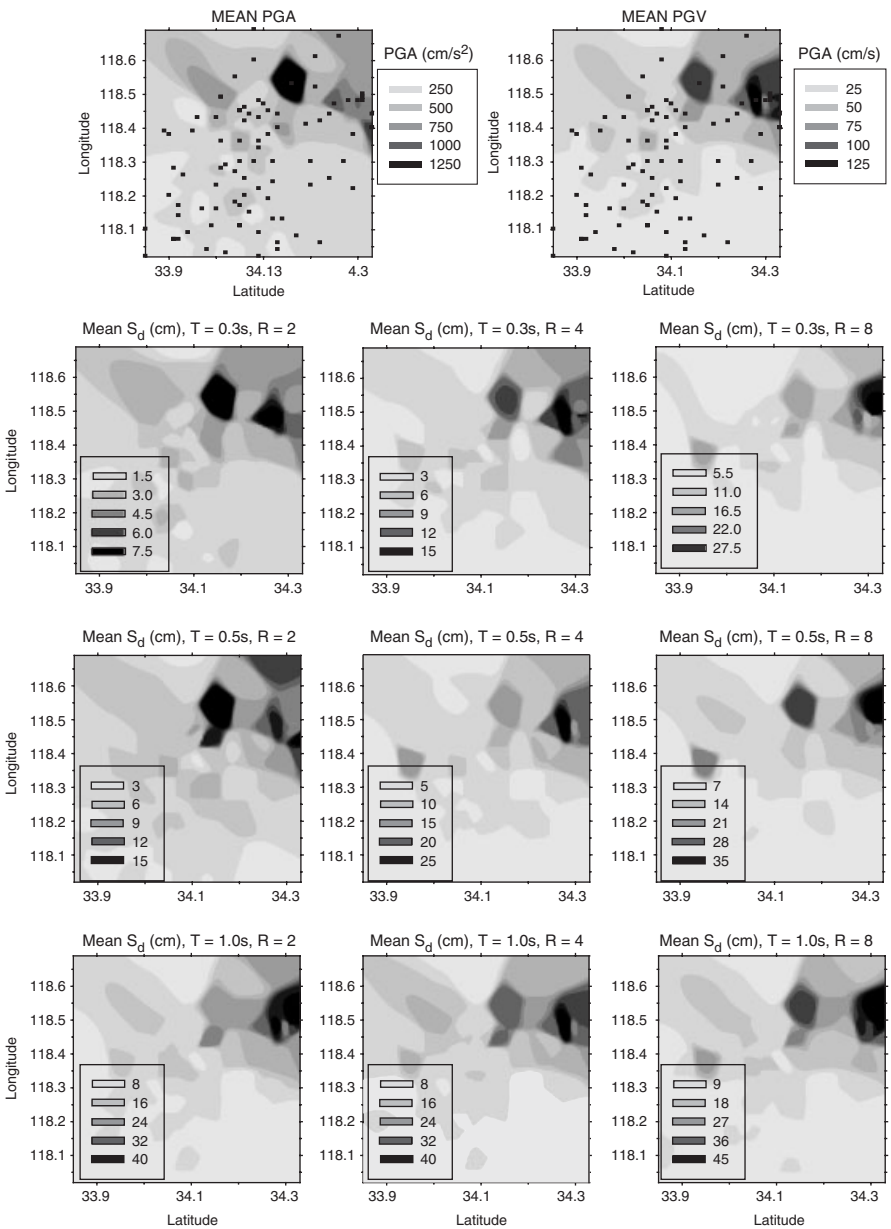

Figure 4. Contour maps for mean horizontal PGA, PGV and corresponding mean inelastic spectral displacements at different periods and R values for the 89 records of the 1994 Northridge earthquake.

also suggest that the overall SDOF deformation demands are more sensitive to the changes in PGV as documented in detail in Figures 2 and 3 using the ground-motion data set of this study.

4.2. Period-dependent correlation of PGV with SDOF deformation demands at different inelastic levels

Using the ground motions presented in this study, the consistency of above observations is tested more comprehensively by computing the period-dependent correlation coefficients (ρ) of PGV for the spectral displacements at different μ and R levels ranging from 1 to 8. Given the pre-defined level of μ or R, the correlation coefficient between spectral displacement $S_d(T_i)$ and PGV at period T_i is calculated for a spectral period range of 0.1–4.0 s. Similar correlation coefficients are also computed for PGA, PGV/PGA ratio and S_a in order to have a fair opinion on the limitations of PGV as an IM on SDOF deformation demands. As summarized in the introductory section, PGA and S_a are widely used IMs in probability-based damage assessment procedures whereas the PGV/PGA ratio is an important ground-motion parameter in various simplified procedures to represent the ground-motion frequency content. This ratio is also introduced as a stable ground-motion parameter correlating well with the non-linear maximum SDOF deformation demands [40]. The comparative results are presented in Figure 5 in which the first column displays the period-dependent correlation coefficients for constant ductility $S_d(T_i)$ and the second column gives the same information at different R levels. The non-linear maximum SDOF deformation demands are computed using the elastoplastic hysteretic model. The results indicate that the PGV intensity measure has significantly higher correlation with spectral displacements at all μ and R levels except for very short periods when compared to the performance of PGA and PGV/PGA intensity measures. The peak ground acceleration reveals a good correlation at very short periods for structures behaving elastically or almost responding in the elastic range. As the level of inelastic deformation increases and the period shifts towards larger values, PGA correlates poorly with the SDOF deformation demand. These comments follow a similar pattern to the ones made for Figure 4. The period-dependent correlation coefficients of PGA also show a more dispersive behaviour for SDOF deformation demands of constant R. The peak ground velocity to acceleration ratio shows a fairly good correlation with SDOF deformation demands when vibration periods are longer than 1.0 s. The correlation is still lower than those of PGV and the use of this particular intensity measure for periods shorter than 1.0 s might result significantly poor and deceiving relations for the assessment of deformation demands on SDOF systems. Similar to the remarks made for PGA the correlation coefficients computed for the PGV/PGA ratio display more scatter for SDOF deformation demands of normalized strength ratio R. The spectral acceleration resembles significantly good correlations with SDOF deformations computed for constant displacement ductility ratios. The correlation coefficients take relatively smaller values as the level of μ increases and when the period shifts towards shorter spectral regions. Nevertheless, they still agree well with the SDOF deformation demands and yield better results with respect to those computed for PGV particularly at periods of vibration less than 0.3 s and greater than 3.0 s. The fairly good performance of S_a is not observed when the deformation demands are computed for normalized strength ratio R. The correlation between S_a and SDOF deformation demands reduces significantly in this particular case especially at shorter periods with increasing levels of R. It should be noted that S_a as an intensity measure gives one-to-one correlation with elastic SDOF deformation demands regardless of the period of vibration; an expected phenomenon due to their direct relation with each other (i.e. $S_a = 4\pi^2/T^2 \times S_{d,e}$ where $S_{d,e}$ is the maximum elastic SDOF deformation demand). The statistical results highlighted in Figure 5 conclude that the observations made on PGV in the

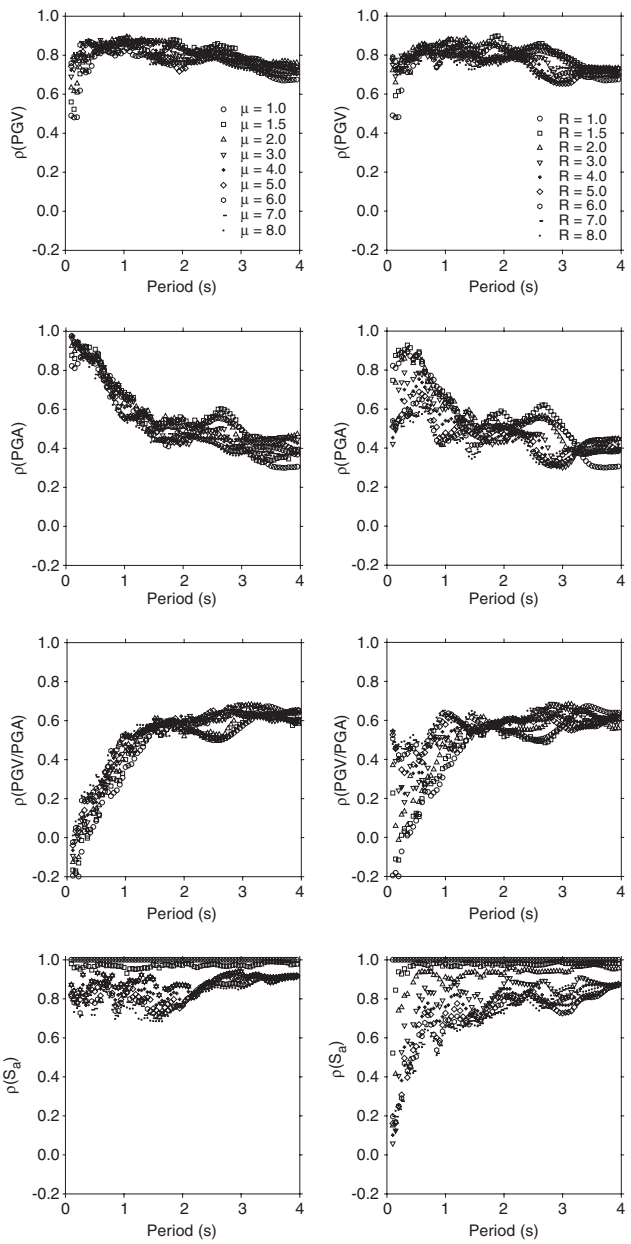

Figure 5. Period-dependent correlation of PGV, PGA, PGV/PGA and S_a with SDOF deformation demand.

previous sections are consistent for the non-linear SDOF deformation demands. Both PGA and PGV/PGA ground-motion parameters have limitations in reflecting the actual variation in deformation demand level when compared to the performance of PGV. Moreover, PGV

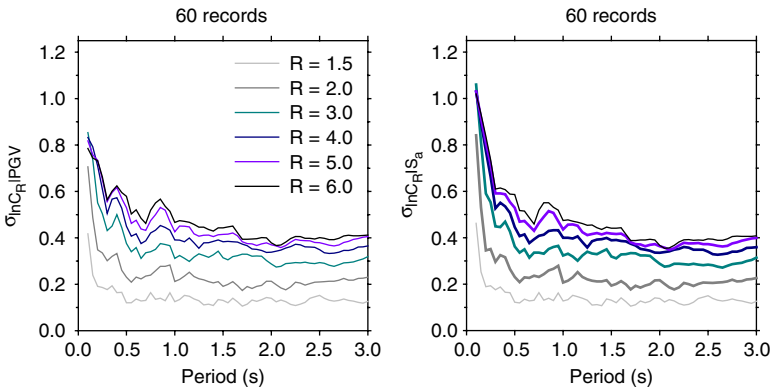

Figure 6. Dispersion on C_R conditioned to PGV and S_a.

draws a more stable correlation with deformation demands as compared to S_a, especially for inelastic, short-period structures. Thus, the intensity measure PGV is more competent with respect to these alternative IMs for seismic design and performance assessment of structures using SDOF response.

4.3. Effect of PGV in reducing the dispersion about the central tendency of SDOF deformation demands

Figure 6 shows the role of PGV on the uncertainty associated with the SDOF deformation demands due to record-to-record variability. The plots in Figure 6 present the comparative dispersion statistics of C_R (maximum inelastic to elastic SDOF deformation ratio for constant R levels [16]) conditioned to PGV and S_a to evaluate the efficiency of these two IMs in reducing the dispersion around the central tendency of DM. Based on the correlation statistics presented in Figure 5, S_a proves to be as competent as PGV in capturing the variation in SDOF deformation demands at different inelastic levels. The dispersions are computed following the 'direct method' procedure described in Reference [21]. This method measures the second moment of actual C_R around the average curve obtained from linear regression in log–log space between C_R and the intensity measure under consideration. For a particular period T_i

$$E[\ln(C_R)|\mathrm{IM}] = \ln(a) + b\,\ln(\mathrm{IM}) \tag{1}$$

computes the expected values of C_R where the regression constants a and b are computed from linear regression analysis in log–log space. The second moment of actual C_R values is given by

$$\sigma_{\ln C_R|\mathrm{IM}} = \sqrt{\frac{\sum(\ln(C_R) - \ln(a \cdot \mathrm{IM}^b))^2}{k-2}} \tag{2}$$

where k is the total number of data points, which is 60 for this study at each particular period T_i. Equations (1) and (2) are repeated for specific oscillator periods ranging from 0.1

to 4.0 s with increments of 0.05 s. The results presented in Figure 6 reveal that PGV and S_a yield comparable performance for spectral periods approximately greater than 0.5 s and for all R values presented. However, the efficiency of S_a in reducing dispersion with respect to PGV loosens for periods less than 0.5 s and particularly when normalized strength ratios attain larger values. These observations are parallel to the discussions concerned on S_a and PGV that are presented in Section 4.2. A similar observation about the efficient role of PGV in reducing the dispersion around the central tendency of SDOF deformation demands is used by Akkar and Miranda [41] to propose a simplified procedure for the deformation demand estimation of short-period SDOF systems.

The measure of dispersion presented in Equations (1) and (2) is not the most appealing method as indicated in Reference [21]. However, it can still provide valuable information in a comparative manner for PGV and S_a intensity measures in reducing the dispersion on the mean SDOF deformation demands. A more elaborate method for this purpose is also presented in Reference [21] by means of the Total Probability Theorem.

4.4. Effect of PGV on stiffness degrading hysteretic behaviour

Previous studies concluded that unless dominant strength deterioration is exhibited by the hysteretic model, the deformation demands computed by the elastoplastic hysteretic model describe an upper bound for general non-linear behaviour [7, 11, 42]. This observation is explored in terms of PGV as the studies cited above described their results for ground motions classified for a specific site or the records were chosen randomly to see the diverse effect of ground motions on structural response. Figure 7 shows the PGV effect on the variation of SDOF deformation demands for different hysteretic models by computing the period-dependent maximum deformation ratios of elastoplastic hysteretic model to those of the modified Clough and modified Takeda models (typical stiffness degrading models with no strength deterioration). The first row in Figure 7 presents the period-dependent mean variation of this ratio for the modified Clough model at different levels of μ whereas the second row shows the same information for modified Takeda in terms of normalized strength values. The plots indicate that the deformation demands on SDOF systems due to different hysteretic models are sensitive to the changes in PGV level. On average, deformation demands computed by the non-degrading elastoplastic model are significantly higher than those of the modified Clough and Takeda for the ground-motion bin with PGV <20 cm/s. The exception is periods of vibration less than 0.5 s where the deformation demands computed by modified Clough and Takeda models take larger values with respect to the elastoplastic model. This observation is valid for the modified Takeda model at all levels of R whereas the SDOF deformation demands by modified Clough are greater than those of the elastoplastic model only for large values of μ. The increase in PGV level decreases the dominancy of inelastic deformation demands computed by the elastoplastic model. On an average, the oscillator deformations computed by the non-degrading elastoplastic model are still higher than those computed by the stiffness degrading models for periods larger than 1.0 s. However, the deformation demands computed by the stiffness degrading models attain larger values with respect to those of elastoplastic behaviour for periods approximately less than 1.0 s especially when PGV >40 cm/s. The larger short-period deformations due to stiffness degradation with respect to non-degrading elastoplastic behaviour are more notable for the modified Takeda model and normalized strength ratio R. This observation indicates that the generic use of the elastoplastic model

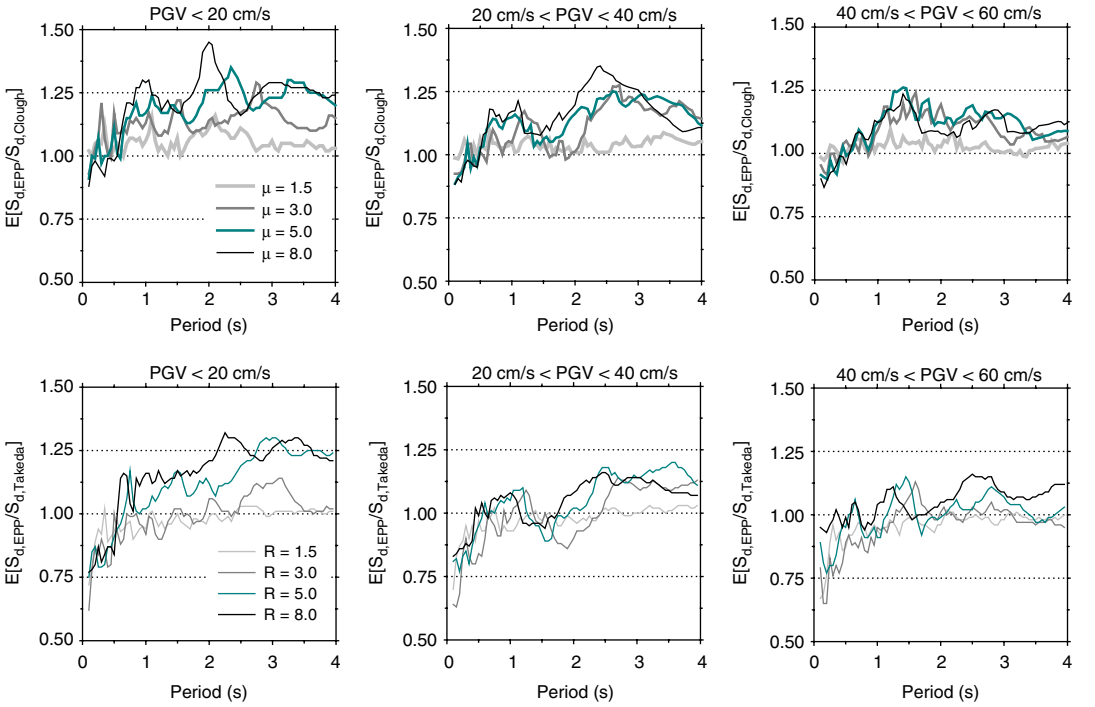

Figure 7. Period-dependent maximum SDOF deformation ratios of non-degrading (elastoplastic) to stiffness degrading (modified Clough and Takeda) hysteretic models at different PGV levels.

to represent the deformation demands at short-period SDOF systems might be misleading particularly when the structural behaviour is represented by the modified Takeda model. The spectral region where the modified Takeda displacements govern to those of the elastoplastic model widens towards longer periods as PGV and level of inelasticity increase.

5. SUMMARY AND CONCLUSIONS

Salient features of PGV intensity measure are examined for non-linear deformation demands on SDOF systems and for some specific ground-motion features that can be effective in structural response. A total of 60 soil site records with $2.5\,\text{km} \leqslant d \leqslant 23\,\text{km}$ and $5.5 \leqslant \mathbf{M} \leqslant 7.6$ is divided into three equal sub-groups covering PGV intervals of less than 20, 20–40 and 40–60 cm/s to achieve the objectives in this study. The records do not exhibit pulse signals that are mostly observed in the near-fault records with forward directivity. This is to prevent biased results due to the particular pulse effect on structural response and ground-motion parameters. Therefore, the results and conclusions of this study are not applicable to such ground motions. The non-linear response history analyses are conducted using non-degrading and stiffness degrading hysteretic behaviours for constant μ and R levels to have a broader sense of understanding about the PGV influence on SDOF deformation demands.

The results presented in this study indicate that the PGV intensity measure correlates well with the earthquake magnitude, effective ground-motion duration and frequency content of ground motions that can provide information for the variation of deformation demands on SDOF systems. The increase in PGV values is associated with an increase in earthquake magnitude and effective duration of records. The frequency composition of ground motions systematically becomes richer in the long period range for increasing PGV.

The statistical results presented for the mean spectral displacements at different inelastic levels show a consistently increasing trend for ground motions of higher velocity. This observation is re-confirmed through a totally independent ground-motion data set from the 1994 Northridge earthquake. The mean spectral displacement statistics at different PGV levels also reveal that the spectral region where the inelastic deformations are significantly higher than their elastic counterparts is sensitive to the amplitude of ground velocity. This spectral region shifts towards longer periods with the increase in PGV. This observation might be a concern for structures whose fundamental periods are within the bounds of this spectral region as they would be more susceptible to structural damage due to the increased deformation demand when they are subjected to higher ground velocity events. These remarks are compatible with the comments made for the relationships between PGV and ground-motion parameters investigated within the context of this study and strengthen the conclusion that PGV is a proper intensity measure candidate for deformation demands on SDOF systems. The validity of these observations is also tested for PGA and PGV/PGA ratio by computing the period-dependent correlation coefficients at different inelastic deformation levels. The comparisons of correlation coefficients between PGV and these two alternative intensity measures once more highlight the superiority of PGV with respect to these two IMs for the seismic design and evaluation of existing structures that deform beyond their elastic limits. Similarly, correlation coefficients computed for spectral acceleration IM do not resemble a stable behaviour particularly for deformations demands computed for $R > 1.5$ when compared to the general performance of correlation coefficients computed for PGV. The dispersion statistics also reveal a better performance of PGV with respect to S_a particularly when the short-period SDOF demands are conditioned on PGV rather than on S_a. The comparative statistics based on the ratios of stiffness degrading hysteretic models to elastoplastic (non-degrading) model showed that the generic use of elastoplastic behaviour in representing the overall SDOF deformation demands should be done with caution by considering the level of PGV especially for short-period structures to prevent undesirable results on structural performance. In brief, future seismological and engineering research on seismic hazard assessment and performance-based seismic design can make use of this IM for more elaborate procedures to assess the seismic vulnerability of structures in earthquake prone zones.

ACKNOWLEDGEMENTS

The authors express their sincere gratitude to Dr Ahmet Yakut and Dr Altuğ Erberik who gave valuable suggestions for the improvement of discussions presented in this study. The constructive comments of two anonymous reviewers and Dr M. Semih Yücemen have increased the quality of the manuscript significantly. Ground motion records used in this study are downloaded from the COSMOS web site. The authors acknowledge the efforts of contributing agencies to this consortium in installing, maintaining and operating the seismic instruments as well as the dissemination of processed data.

REFERENCES

1. Veletsos AS, Newmark NM. Design procedures for shock isolation systems of underground protective structures. *Report No. RTD TDR-63-3096*, Air Force Weapons Laboratory, New Mexico, 1964.
2. Newmark NM, Hall WJ. Seismic design criteria for nuclear reactor facilities. *Report No. 46*, Building Practices for Disaster Mitigation, National Bureau of Standards, U.S. Department of Commerce, 1973; 209–236.
3. Newmark NM, Hall WJ. *Earthquake Spectra and Design*. EERI Monograph Series, Earthquake Engineering Research Institute: Oakland, CA, 1982.
4. Lai SP, Biggs JM. Inelastic response spectra for aseismic building design. *Journal of Structural Division* 1980; **106**:1295–1310.
5. Elghadamsi F, Mohraz B. Inelastic earthquake spectra. *Earthquake Engineering and Structural Dynamics* 1987; **15**:91–104.
6. Riddell R, Newmark NM. Statistical analysis of the response of nonlinear systems subjected to earthquakes. *Structural Research Series No. 468*, Department of Civil Engineering, University of Illinois, Urbana, 1979.
7. Riddell R, Hidalgo P, Cruz E. Response modification factors for earthquake resistant design of short period structures. *Earthquake Spectra* 1989; **5**:571–590.
8. Riddell R, Garcia JE, Garces E. Inelastic deformation response of SDOF systems subjected to earthquakes. *Earthquake Engineering and Structural Dynamics* 2002; **31**:515–538. DOI: 10.1002/eqe.142.
9. Nassar AA, Krawinkler H. Seismic demands for SDOF and MDOF systems. *Report No. 95*, The John A. Blume Earthquake Engineering Center, Stanford University, CA, 1991.
10. Miranda E. Seismic evaluation and upgrading of existing buildings. *Ph.D. Thesis*, University of California, Berkeley, CA, 1991.
11. Miranda E. Site dependent strength reduction factors. *Journal of Structural Engineering* 1993; **119**:3503–3519.
12. Vidic T, Fajfar P, Fischinger M. Consistent inelastic design spectra: strength and displacement. *Earthquake Engineering and Structural Dynamics* 1994; **23**:507–521.
13. Ordaz M, Pérez-Rocha LE. Estimation of strength-reduction factors for elasto-plastic systems: a new approach. *Earthquake Engineering and Structural Dynamics* 1998; **27**:889–901. DOI: 10.1002/(SICI)1096-9845(199809)27.
14. Cuesta I, Aschheim MA. Isoductile strengths and strength reduction factors of elasto-plastic SDOF systems subjected to simple waveforms. *Earthquake Engineering and Structural Dynamics* 2001; **30**:1043–1059. DOI: 10.1002/eqe.51.
15. Miranda E. Inelastic displacement ratios for structures on firm sites. *Journal of Structural Engineering* 2000; **126**:1150–1159.
16. Ruiz-García J, Miranda E. Inelastic displacement ratios for evaluation of existing structures. *Earthquake Engineering and Structural Dynamics* 2003; **32**:1237–1258. DOI: 10.1002/eqe.271.
17. Farrow KT, Kurama A. SDOF demand index relationships for performance-based seismic design. *Earthquake Spectra* 2004; **19**:799–838.
18. Shome N, Cornell CA, Bazzuro P, Carballo E. Earthquake, records and nonlinear response. *Earthquake Spectra* 1998; **14**:469–499.
19. Cordova PP, Deierlein GG, Mehanny SS, Cornell CA. Development of a two-parameter seismic intensity measure and probabilistic assessment procedure. *Proceedings of the 2nd U.S.–Japan Workshop on Performance-based Earthquake Engineering for Reinforced Concrete Building Structures*, Sapporo, Japan, 11–13 September 2000.
20. Krawinkler H, Medina R, Alavi B. Seismic drift and ductility demands and their dependence on ground motions. *Engineering Structures* 2003; **25**:637–653.
21. Giovenale P, Cornell CA, Esteva L. Comparing the adequacy of alternative ground motion intensity measures for the estimation of structural response. *Earthquake Engineering and Structural Dynamics* 2004; **33**:951–979. DOI: 10.1002/eqe.386.
22. Wald DJ, Quitoriano V, Heaton TH, Kanomori H. Relationships between peak ground acceleration, peak ground velocity and modified Mercalli intensity in California. *Earthquake Spectra* 1999; **15**:557–564.
23. Wu YM, Teng TI, Shin TC, Hsiao NC. Relationship between peak ground acceleration, peak ground velocity and intensity in Taiwan. *Bulletin of the Seismological Society of America* 2003; **93**:386–396.
24. Anderson JC, Bertero VV. Uncertainties in establishing design earthquakes. *Journal of Structural Engineering* 1987; **113**:1709–1723.
25. Uang CM, Bertero VV. Implications of recorded earthquake ground motions on seismic design of building structures. *Report No. UCB/EERC-88/13*, Earthquake Engineering Research Center, University of California, Berkeley, CA, 1988.
26. Joyner WB, Boore DM. Peak horizontal acceleration and velocity from strong-motion records including the records from the 1979 Imperial Valley, California, earthquake. *Bulletin of the Seismological Society of America* 1981; **71**:2011–2038.
27. Campbell KW. Near-source attenuation of peak horizontal acceleration. *Bulletin of the Seismological Society of America* 1981; **71**:2039–2070.

28. Campbell KW. Strong motion attenuation relations: a ten-year perspective. *Earthquake Spectra* 1985; **1**: 759–804.
29. Sabetta F, Pugliese A. Estimation of response spectra and simulation of nonstationary earthquake ground motions. *Bulletin of the Seismological Society of America* 1996; **86**:337–352.
30. Abrahamson N, Silva W. Empirical response spectra relations for shallow crustal earthquakes. *Seismological Research Letters* 1997; **68**:94–127.
31. Tromans IJ, Bommer JJ. The attenuation of strong motion peaks in Europe. *12th European Conference on Earthquake Engineering*, London, Paper No. 394, 2002.
32. Theodulidis NP, Papazachos BC. Dependence of strong ground motion on magnitude-distance, site geology and macroseismic intensity for shallow earthquakes in Greece: I, peak horizontal acceleration, velocity and displacement. *Soil Dynamics and Earthquake Engineering* 1992; **11**:387–402.
33. Boatwright J, Bundock H, Leutgert J, Seekins L, Gee L, Lombard P. The dependence of PGA and PGV on distance and magnitude influence inferred from Northern California shakemap data. *Bulletin of the Seismological Society of America* 2003; **93**:2043–2055.
34. International Conference of Building Officilas (ICBO). *International Building Code*. Whittier: CA, 2000.
35. Iwan WD, Huang CT, Guyader AC. Important features of the response of inelastic structures to near-field ground motion. *12th World Conference on Earthquake Engineering*, Auckland, New Zealand, Paper No. 1740, 2000.
36. Somerville PG, Smith NF, Grawes RW, Abrahamson NA. Modification of empirical strong ground motion attenuation relations to include the amplitude and duration effects of rupture directivity. *Seismological Research Letters* 1997; **68**:199–222.
37. Bommer JJ, Martínez-Periera A. The effective duration of earthquake strong motion. *Journal of Earthquake Engineering* 1999; **3**:127–172.
38. Mahin SA, Lin J. Construction of inelastic response spectra for single degree of freedom systems. *Report No. UCB/EERC-83/17*, Earthquake Engineering Research Center, University of California at Berkeley, CA, 1983.
39. Otani S. Inelastic analysis of RC frame structures. *Journal of Structural Division* 1974; **100**:1433–1449.
40. Zhu TJ, Tso WK, Heidebrecht AC. Effect of peak ground a/v ratio on structural damage. *Journal of Structural Engineering* 1988; **114**:1019–1037.
41. Akkar S, Miranda E. Improved displacement modification factor to estimate maximum deformations of short period structures. *13th World Conference on Earthquake Engineering*, Vancouver, BC, Canada, Paper No. 3424, 2004.
42. Foutch DA, Shan S. Effects of hysteresis type on the seismic response of buildings. *Sixth U.S. National Conference on Earthquake Engineering*, Seattle, Washington, DC, Paper No. 409, 1998.

